ISSN 2007-9737

Binary Coronavirus Disease Optimization Algorithm for Spectral Band Selection

Seyyid Ahmed Medjahed[1,*], Fatima Boukhatem[2]

[1] Univeristy of Relizane,
Algeria

[2] Univeristy of Djilali Liabes, Sidi Belabes,
Algeria

seyyidahmed.medjahed@univ-relizane.dz, fatima.boukhatem@univ-sba.dz

Abstract. Remote sensing has become a very interesting tool in various applications because its ability to capture detailed spectral information with a wide range of wavelengths. However, the large dimensionality of hyperspectral image and the inherent complexity provides many challenges for image classification and the accuracy rate. One of the critical preprocessing step in wealth of data hyperspectral image classification is the spectral band selection which play a very important role to reduce the dimensionality and by consequences reduce the Huge phenomena. In this paper, we propose a new spectral band selection approach based on a new metaheuristic called Coronavirus Disease Optimization Algorithm (COVIDOA). A binary version of this metaheuristic is proposed with a new objective function based on accuracy rate and distance measure. The proposed approach will be tested on three hyperspectral images widely used in the literature and demonstrating its efficacy in improving classification accuracy rate.

Keywords. Band selection, coronavirus disease, optimization algorithm, classification, hyperspectral image.

1 Introduction

In earth observation and remote sensing, hyperspectral imaging has become a vital tool in various applications. It offers a wealth of data provided by the detailed spectral information. These data can be exploited for many applications such as agriculture, environmental monitoring, mineral exploration, military, etc. Unfortunately, the large dimensionality and the complexity of hyperspectral image presents a big challenge for classification and feature extraction [9].

Spectral band selection is the important step in the hyperspectral image classification and analysis. It aims to improve the efficiency and accuracy of classification algorithms by selecting only the most informative bands, enhancing signal-to-noise rations and reducing computational complexity.

In general, spectral band selection (feature selection) methods are categorized in three categories: Filter, Wrapper and Embedded [11, 14]. Filter approaches are a type of feature selection that evaluates the relevance of each feature independently of the classifier (machine learning model). They use statistical methods to calculate the rank of individual features. Wrapper approaches are a feature selection approach that use the classifier to evaluate the subset of features [1, 4]. Embedded approaches incorporate feature selection into the process of training of a machine learning model.

To address the problem of spectral band selection, researchers have used the power of metaheuristic optimization techniques. In the

context of hyperspectral image classification, the metaheuristic spectral band selection methods can help to efficiently select the optimal subset of bands by searching through the vast spectrum of possible band combinations and identify the subset spectral band that best serve the classification [10, 7].

Numerous researches have been done in the context of band selection. In [15], the authors proposed an unsupervised band selection for medical images analysis based on the data gravitation and weak correlation. In [12], Yujuan Sun et al., propose a new band selection based on hyperspectral piling Ficher graphs (HSPFiGs) by constructing a band selection optimization method. Reza Aghaee et al. [2], propose a fusion based approach using metaheuristic band selection. In [13], a graph regularized spatial-spectral subspace slusteringt method is proposed for band selection. It adopts superpixel segmentation to preserve the spatial information. Medjahed et al. [8] used the Salp Swarm Algorithm with Threshold accepting for band selection and a new objective functions are tested.

In this paper, a new approach for spectral band selection in hyperspectral image classification is proposed. This approach is based on a new objective function composed of two terms: the first one is the classification accuracy rate and the second term is the distance measure. The aim of this work is to select the optimal spectral band which improves the classification accuracy rate and reduce the dimensionality of the problem.

The proposed approach is called SBS-BCDOA (Spectral Band Selection - Binary Coronavirus Disease Optimization Algorithm) and it is based on Coronavirus Disease Optimization Algorithm which is a new meta-heuristic inspired on the movement and search of the corona-virus among different societies. A binary version of Coronavirus Disease Optimization Algorithm is proposed.

To assess the effectiveness of the proposed approach, we consider three commonly utilized hyperspectral images widely used in the literature i.e. Salinas, Pavia University and Indian Pines.

The rest of paper is organized as follows: In the next section, we present the proposed approach SBS-BCDOA. Following this, we present the results of our study and discuss them. Lastly, we conclude our study by summarizing this work and presenting some perspectives.

2 Proposed Approach SBS-BCOVIDOA

2.1 Problem Formulation

The aims of this work is to address the problem of spectral band selection in hyperspectral image classification. The problem of band selection can be modeled as a combinatorial optimization problem. Let assume $B = \{b_1, \ldots, b_n\}$ a set of spectral band and $X = \{x_1, \ldots, x_n\}$ is a binary vertoc. The problem is designed as follows:

$$x_i = \begin{cases} 1 \text{ if } b_i \text{ is selected,} \\ 0 \text{ if } b_i \text{ is not selected.} \end{cases} \quad (1)$$

The fundamental concept of band selection is to identify the most favorable band subset that improve significantly the classification accuracy rate. The basic idea of this study, is to propose a binary version of Coronavirus Disease optimization algorithm and adapt it to the combinatorial optimization problem which is a binary optimization.

2.2 Coronavirus Disease Optimization Algorithm

In the CVSO algorithm, an initial population is randomly created and this population is divided into groups called "*typical societies*". The best member of each society serves as a proxy for the individual spreading the coronavirus in that society. The rest of the population is referred to as the citizen of the society and it includes individuals who can learn from their social interactions and have ability to move between societies. The initial population (N_p) is divided into N_v society and each society has N_p/N_v members. The best one is called V (Virus) and the rest is called H (Human) [5]. The CVSO algorithm is composed of three steps :

2.2.1 First Step

The first step is referred to as the spread phase which contains four events that take place within each society. These events are: Spread of the virus, virusization of individuals, strengthening of people, the death and birth of new virusize individuals. The best member in society is the virus or the individual infected by the virus. For the n^{th} individual in the i^{th} society, we have the following equation:

$$H_n^{new} = V_i + \xi \times (V_i - H_n^{old}), \tag{2}$$

where, ξ provides random number between $[0, 1]$ equal to the dimesion number of the problem (in our study is the number of initial spectral band).

From the equation 2, we notice that the virus try to infect the individual. A small value means that the individual is stronger and effective in the optimization (case of minimization). The strength of the individual represents the objective function in the optimization problem which is the $Cost(H)$. In the other side, if the power of the n^{th} individual from the i^{th} society is in safe place (safe distance), he/she will be less affected by the virus V^i, and the equation of social learning will be as follows [5]:

$$H_n^{new} = H_n^{old} + \xi \times (V_i - H_n^{old}). \tag{3}$$

The safe distance is designed in the fact that if the individual is strong to compete with the virus agent, the function of the individual $(Cost(H_n))$ should not be much greater than the value of virus agent $(Cost(V_i))$ and equal to $1 + \left|R1^{Iter}\right|$. The safe margin is defined as follows [5]:

$$\begin{gathered}\text{if } Cost(H_n) < (1 + \left|R1^{iter}\right|) \times Cost(V_i) \text{ then} \\ H_n^{new} = H_n^{old} + \xi \times (V_i - H_n^{old}) \\ \text{else} \\ H_n^{new} = V_i + \xi \times (V_i - H_n^{old}) \\ \text{end},\end{gathered} \tag{4}$$

where, H_n^{new} is the new position of the nth individual. R1 is a random value using normal distribution. This individual can find a new position, die and a new individual will be created. This can be described as follows [5]:

$$\begin{gathered}\text{if } Cost(H_n^{new}) < Cost(H_n^{old}) \text{ then} \\ H_n = H_n^{new} \\ \text{else if } \xi < Kd \\ H_n = H_{min} + \xi \times (X_{\max} - X_{min}) \\ \text{else} \\ H_n = H_n^{old} \\ \text{end},\end{gathered} \tag{5}$$

where kd is the probability of individual death and the birth of a new individual with random position [5].

2.2.2 Second Step

The second step is the evolution phase. The viruses can become stronger over time. This evolution can be defined as follows [5]:

$$V_i^{new,k} = V_i + \frac{\xi}{Iter} \times (R2) \tag{6}$$

where V_i is the i^{th} virus. This equation 6 represents the evolution of the virus to be stronger. $R2$ is a random value using normal distribution. The algorithm can be improved by avoiding the local optimal as follows [5]:

$$\begin{gathered}\text{for } k = 1 : N_e \\ V_i^{new,k} = V_i + \frac{\xi}{Iter} \times (R2) \\ \text{if } Cost(V_i^{new,k}) < Cost(V_i) \\ V_i = V_i^{new,k} \\ \text{end} \\ \text{end},\end{gathered} \tag{7}$$

where N_e is the number of evolutionary cycle which can be defined by the user.

2.2.3 Third Step

The third step is the travel phase which allows to the individuals of each society to randomly migrate to another society and spread the virus. As the real world, people can travel and spread the virus. In CVSO algorithm, in each iteration, we select randomly individuals (H) from each society which is a $SubSociety$ and each society can randomly accept the individuals [5].

A random individuals can migrate from the m^{th} society to i^{th} society, and a random number of individuals can migrate from the i^{th} society to the n^{th} society. This migration is illustrated on the following equation [5]:

$$N_t(i) = round((\xi \times (1 - \xi)) \times N_h(I)), \quad (8)$$

where N_t is the number of immigrants and N_h is the number of individuals in that society.

The algorithm stops when the user performs the desired iteration number or when the global optimal is the solution [5].

The pseudocode of the algorithm is described in Algorithm 1 [5].

2.3 Binary Coronavirus Disease optimization algorithm

A binary version of Coronavirus Disease optimization algorithm is proposed for band selection. The optimal solution is a binary vector with the following condtion, if $x = 1$ the band is selected and it will be part of the machine learning model otherwise $x = 0$ the band is not selected. To take account the binary version, we propose to use the Hyperbolic Tangent function that maps continuous values.

You can then map the values to 0 or 1 based on whether they are greater or less than 0:

$$\begin{cases} H(x_i) = 1 \text{ if } \tanh(x_i) > 0, \\ H(x_i) = 0 \text{ if } \tanh(x_i) \leq 0\ . \end{cases} \quad (9)$$

2.4 Objective Function

In wrapper method and in most cases, the objective function is typically defined in terms of either the error rate or the classification accuracy rate. We propose an objective function with two terms, the first term is the classification accuracy rate and the second term is the capability of feature discrimination.

Algorithm 1 Coronavirus Disease Optimization Algorithm [5]

initialization
for $i = 1 : N_P$ **do**
  $H_i = X_{min} + \xi \times (X_{max} - X_{min})$
end for
$H = sort(H)$;
for $i = 1 : N_V$ **do**
  $V_i = H_i$
end for
for $i = 1 : N_V$ **do**
  $Society(i) = [V_i, H(l : N_h(i))]$
  $H = H((N_h(i) + 1) : N_p)$
end for
Process of the algorithm and check fitness
for $i = 1 : N_V$ **do**
  for $n = 1 : N_h(i)$ **do**
    if $Cost(H_n) < (1 + \left|R1^{Iter}\right|) \times Cost(V_i)$ **then**
      $H_n^{new} = H_n^{old} + \xi \times (V_i - H_n^{old})$
    else
      $H_n^{new} = V_i + \xi \times (V_i - H_n^{old})$
    end if
    if $Cost(H_n^{new}) < Cost(H_n^{old})$ **then**
      $H_n = H_{new}^n$
    else if $\xi < Kd$ **then**
      $H_n = X_{min} + \xi \times (X_{\max} - X_{min})$
    else
      $H_n = H_n^{old}$
    end if
  end for
end for
Changing the virus agent position
for $i = 1 : N_v$ **do**
  if $BestCost(H) < Cost(V_i)$ **then**
    $V_i = Best(H)$
  end if
end for
Evaluating the fitness
for $i = 1 : Nv$ **do**
  for $k = I : N_e$ **do**
    $V_i^{new,k} = V_i + \frac{\xi}{Iter} \times (R2)$
    if $Cost(V_i^{new,k}) < Cost(V_i)$ **then**
      $V_i = V_i^{new,k}$
    end if
  end for
end for
Carry out the migration phase on the citizens of the societies
$N_t(i) = round((\xi \times (1 - R2)) \times N_h(i))$
$SubSociety(i) = Human((N_h(i) - N_t(i) + 1) : N_h(i))$
for $i = 1 : N_v$ **do**
  $N_h(i) = N_h(i) - N_t(i)$
  $Society(i) = Society(i) - SubSociety(i)$
end for
for $i = 1 : N_V$ **do**
  $N_h(i) = N_h(i) + N_t(j)$
  $j = 1 : N_v - \{i\}$
  $Society(t) = Society(i) + SubSociety(j)$
end for

2.4.1 First Term

The first term of the objective function is the classification accuracy rate. The goal is to maximize the rate of the accuracy. The proposed idea is to use three classifiers: Support Vector Machine (SVM), Random Forest (RF) and Naïve Bayes (NB). We will compute the average of classification accuracy rate produced by the three classifiers to avoid having a subset of features which are totally dependent of a specific classifier:

$$f_1(X,B) = \frac{car_{SVM}(X,B) + car_{RF}(X,B) + car_{NB}(X,B)}{3} \tag{10}$$

where,

$car_{SVM}(X,B)$, is the classification accuracy rate provided by SVM.

$car_{RF}(X,B)$, is the classification accuracy rate provided by RF.

$car_{NB}(X,B)$, is the classification accuracy rate provided by NB.

2.4.2 Second Term

The second term of the objective function is the score of spectral band discrimination. The basic idea is to calculate the power of feature discrimination using Jeffries-Matusita distance. The Jeffries-Matusita (JM) distance is a statistical measure used to quantify the separability of features in supervised classification. It measures the dissimilarity between two classes in feature distribution [6].

The Jeffries-Matusita distance between two classes is defined as follows:

Let's i and j two classes, the Jeffries-Matusita distance between the class i and class j for a feature is described as follows:

$$JM_{i,j} = \sqrt{2(1 - e^{B_{i,j}})}, \tag{11}$$

where, $B_{i,j}$ is the Bhattacharyya distance [3] defined as follows:

$$B_{i,j} = \frac{1}{8}(m_i - m_j)^T \left(\frac{\sum_i + \sum_j}{2}\right)(m_i - m_j) + \frac{1}{2}\ln\left[\frac{\left|\left(\sum_i + \sum_j\right)/2\right|}{|\sum_i|^{\frac{1}{2}} + \left|\sum_j\right|^{\frac{1}{2}}}\right]$$

where, m is the class mean vectors and $\sum$ is the class covariance. The goal is to find the subset of features that maximize the JM distance, this function can be formulated as follows:

$$Dis_b = \sum_{i=1}^{c}\sum_{j=1}^{c} p(\omega_i)p(\omega_j)JM_{i,j}, \tag{12}$$

where Dis_b is the JM distance for the spectral band b.

$p(\omega)$ is the class prior probabilities and c is the number of classes.

The term of the objective function related to Jeffries-Matusita distance is given by the equation:

$$f_2(X,B) = \frac{1}{N}\sum_{i=1}^{n} x_i \times Dis_{bi}. \tag{13}$$

The final form of the objective function is defined as follows:

$$f(X,B) = \alpha \times f_1(X,B) + \beta \times f_2(X,B). \tag{14}$$

The final goal is to maximize the objective function $f(X,B)$.

3 Experimental Results

3.1 Dataset

To assess the effectiveness of the proposed approach SBS-BCOVIDOA, we carried out the experimentation under three commonly referenced hyperspectral images in the literature: Salinas, Indian Pines, and Pavia University.

3.1.1 Salinas Image

The Salinas image is an hyperspectral image which was taken by the AVIRIS (Airborne Visible InfraRed Imaging Spectrometer) above the Salinas Valley, Southern California, USA. The size of this image is 512×217 pixels contains 224 bands with a spectral range from $0.4\ \mu m$ to $2.5\ \mu m$. There are 16 ground truth classes: Broccoli-green-weeds-1, Broccoli-green-weeds-2, Fallow, Fallow-rough-plow, Fallow-smooth, Stubble, Celery, Grapes-untrained, Soil-vinyard-develop, Corn-senesced-green-weeds, Lettuce-romaine-4wk, Lettuce-romaine-5wk, Lettuce-romaine-6wk, Lettuce-romaine-7wk, Vineyard-untrained and Vineyard-vertical-trellis [9, 8].

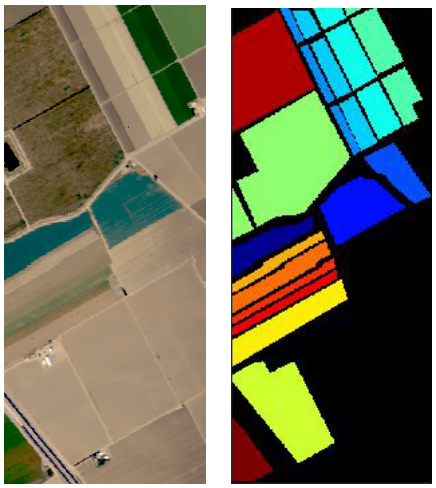

(a) (b)

Fig. 1. Salinas hyperspectral image. (a) Color compose. (b) Ground truth.

3.1.2 Indian Pines Image

Indian Pines, which is the second hyperspectral image used in this experimentation. It wa captured over the agricultural region of Northwestern of Indiana,USA. The size of thi image is 145×145 pixels and it contains 220 bands in the spectral range $0.5\ \mu m$ to $2.5\ \mu m$. It was captured by AVIRIS and it contains 16 ground truth classes: Alfalfa, Corn-notill, Corn-mintill, Corn, Grass-pasture, Grass-trees, Grass-pasture-mowed, Hay-windrowed, Oats, Soybean-notill, Soybean-mintill, Soybean-clean, Wheat, Woods, Buildings-Grass-Trees-Drives, and Stone-Steel-Towers [9, 8].

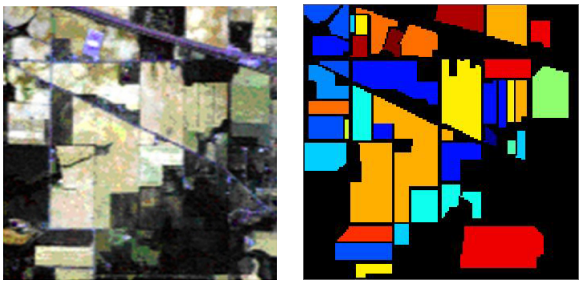

(a) (b)

Fig. 2. Indian Pine hyperspectral image. (a) Color image. (b) Ground truth.

3.1.3 Pavia University Image

Pavia University hyperspectral image was captured over the urban area of Pavia University. The size of this image image is 610×340 pixels and it was collected by ROSIS. It contains 103 bands in the spectral range from $0.4\mu m$ to $0.86\ \mu m$. The ground truth differentiates 9 classes: Asphalt, Meadows, Gravel, Trees, Painted Metal Sheets, Bare Soil, Bitumen, Self-Blocking Bricks, and Shadows [9, 8].

3.2 Parameters Setting

The parameters setting of the proposed approach are as follows.

For the classifiers we used SVM with Gaussian kernel ($\alpha = 0.5$). For the optimization method, the number of iteration is set to 200 with population set to 50. For the objective function, α and β are set to 0.5. These values are taken by experimentation.

As each classifier, we proposed to use 40% of the pixels in the training phase, 30% of the pixed in the validation phase and the remaining 30% are considered for the testing phase.

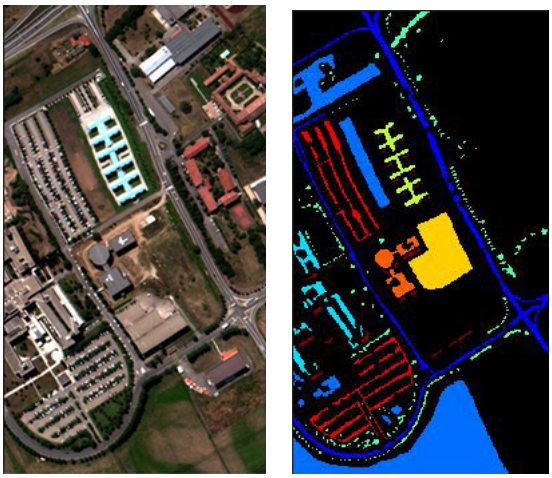

(a) (b)

Fig. 3. Pavia University hyperspectral image. (a) Color Image. (b) Ground truth.

3.3 Results and Discussion

In this section, we present the result obtained by the proposed approach in term of individual class accuracy, average accuracy (AA) and overall accuracy (OA). Note that in the context of images classification, OA and AA are an evaluation metrics of the classification used to summarizing the performance of a classifier. OA produces an overall measure of the classification accuracy rate without considering class imbalances and AA considers the individual accuracies for each class and produces a more balanced assessment.

Table 1 describes the numerical results obtained by the proposed approach and applied on Pavia University, Salinas and Indian Pines hyperspectral images.

The analysis of the results obtained for the Pavia University hyperspectral image, demonstrates promising results. The proposed approach achieved a high coverall accuracy of 90.95%. this measure provides a high-level overview of the classifier's performance across all classes. The robust OA underscores the effectiveness of our methodology in capturing the underlying patterns within the hyperspectral data. Moreover, the AA highlights the reliability of the proposed approach by achieving a notable AA 88.82%. The

Table 1. Classification accuracy rate obtained by WOA-SVM over Salinas scene and compared with previous works.

Class	Proposed Approach SBS-BCDOA		
	Pavia University	Indian Pines	Salinas
#1	89.04	7.14	99.00
#2	98.28	62.54	99.91
#3	76.90	57.22	98.90
#4	87.81	44.05	99.64
#5	99.25	82.06	97.94
#6	73.69	95.66	99.95
#7	86.84	76.47	99.39
#8	87.55	97.90	82.78
#9	100.00	25.00	99.73
#10	-	63.18	94.25
#11	-	76.44	96.56
#12	-	33.70	99.39
#13	-	96.74	97.45
#14	-	95.91	94.23
#15	-	24.13	61.06
#16	-	80.35	98.61
AA	88.82	63.66	94.92
OA	90.95	71.55	90.28

achieved AA of 88.82% indicates that our approach generalizes well across different classes, ensuring consistent and accurate predictions even in the presence of varying class sizes.

For Indian Pines hyperspectral image, the proposed approach yielding an OA of 71.55% which underscores the effectiveness of this approach in capturing the spectral intricacies. The proposed approach indicated an average accuracy of 63.66% across the individual classes. While AA considers the impact of class imbalances, the achieved value of 63.66% suggests that our approach maintains a good balance in performance across different classes, effectively generalizing to various spectral signatures present in the Indian Pines dataset.

The third experimentation was done over the Salinas hyperspectral image. The approach provided an overall accuracy of 90.28% which emphasized the effectiveness of our proposed approach. Furthermore, the AA revealing a good average accuracy of 94.92% across individual classes.

Figures 4, 5 and 6 illustrate the visual results which are the classification map obtained by the

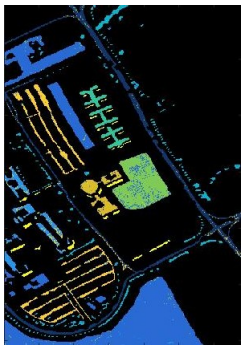

Fig. 4. Classification map obtained by the proposed approach for Pavia University

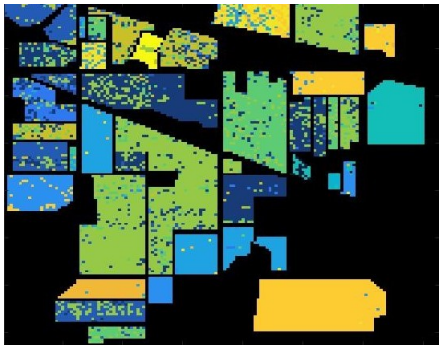

Fig. 5. Classification map obtained by the proposed approach for Indian Pines

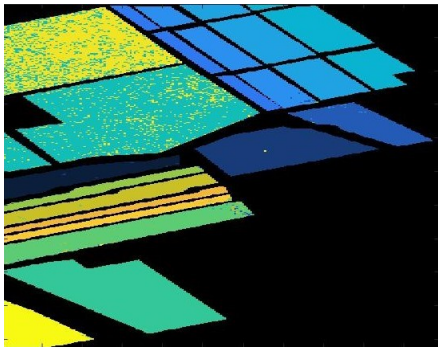

Fig. 6. Classification map obtained by the proposed approach for Salinas

proposed approach. The visual representation of the classification results is a classification map which produces an intuitive understanding of how well our proposed approach performs in distinguishing different classes. The analysis of the classification maps demonstrates that the proposed approach captures the spatial distribution of various classes. The classification maps reveal a clear spatial separation between the classes which indicates that our approach effectively distinguishes between different land cover types. The class assignments are clearly visible and distinguishable on the map, demonstrating the accuracy with which our approach allocates pixels to their respective land cover classes.

4 Conclusion

In this paper, we proposed a new spectral band selection approach based on a new meta-heuristic called Coronavirus Disease Optimization Algorithm which a binary version is proposed and adapted to the problem of band selection. Additionally, we propose a new objective function based on two important terms: The first term is the average classification rate obtained by SVM, RF and NB. The second term is the Jeffries-Matusita distance which is used to compute the capability of a band to separate the classes. The proposed approach is tested under three hyperspectral images widely used in the literature: Pavia University, Indian Pines and Salinas. The performance evaluation of our approach, applied to Indian Pines, Salinas, and Pavia University, reveals consistently high Average Accuracy (AA) and Overall Accuracy (OA). These metrics underscore the robustness and generalization capabilities of our classifier, showcasing its potential applicability in real-world scenarios. Visual interpretation of the classification maps further reinforces the reliability of our results. The well-distinguished regions and clear spatial separation between classes affirm the model's proficiency in capturing intricate spectral patterns, while comparisons with ground truth data validate the accuracy of our classifications. While the proposed approach has demonstrated significant success in term of AA and OA, we propose as future perspective to test the proposed approach in tuning hyperparameters or improve the classification of DNA microarray.

References

1. **(2024).** Advancing gene feature selection: Comprehensive learning modified hunger games search for high-dimensional data. Biomedical Signal Processing and Control, Vol. 87, pp. 105423. DOI: https://doi.org/10.1016/j.bspc.2023.105423.
2. **Aghaee, R., Momeni, M., Moallem, P. (2023).** A fusion-based approach to improve hyperspectral images classification using metaheuristic band selection. Applied Soft Computing, Vol. 148, pp. 110–753. DOI: https://doi.org/10.1016/j.asoc.2023.110753.
3. **Bhattacharyya, A. K. (1936).** On a measure of divergence between two multinomial populations. Sankhya: The Indian Journal of Statistics, Vol. 4, No. 4, pp. 401–406. DOI: 10.2307/25049536.
4. **Dai, J., Huang, W., Zhang, C., Liu, J. (2024).** Multi-label feature selection by strongly relevant label gain and label mutual aid. Pattern Recognition, Vol. 145, pp. 109945. DOI: https://doi.org/10.1016/j.patcog.2023.109945.
5. **Golalipour, K., Faraji Davoudkhani, I., Nasri, S., Naderipour, A., Mirjalili, S., Abdelaziz, A. Y., El-Shahat, A. (2023).** The corona virus search optimizer for solving global and engineering optimization problems. Alexandria Engineering Journal, Vol. 78, pp. 614–642. DOI: https://doi.org/10.1016/j.aej.2023.07.066.
6. **Jeffries, N. (1957).** Some distance properties of latent root and vector methods used in multivariate analysis. Biometrika, Vol. 44, No. 1-2, pp. 239–252. DOI: 10.2307/2333920.
7. **Medjahed, S. A., Ouali, M. (2018).** Svm-rfe-ed: A novel svm-rfe based on energy distance for gene selection and cancer diagnosis. Computacion y Sistemas, Vol. 22, No. 2, pp. 675–683.
8. **Medjahed, S. A., Ouali, M. (2020).** A new hybrid ssa-ta: Salp swarm algorithm with threshold accepting for band selection in hyperspectral images. Applied Soft Computing, Vol. 95, pp. 106–534. DOI: https://doi.org/10.1016/j.asoc.2020.106534.
9. **Medjahed, S. A., Saadi, T. A., Benyettou, A., Ouali, M. (2016).** Gray wolf optimizer for hyperspectral band selection. Applied Soft Computing, Vol. 40, pp. 178–186.
10. **Medjahed, S. A., Saadi, T. A., Benyettou, A., Ouali, M. (2017).** Kernel-based learning and feature selection analysis for cancer diagnosis. Applied Soft Computing, Vol. 51, pp. 39–48.
11. **Sewwandi, M. A. N. D., Li, Y., Zhang, J. (2023).** Granule-specific feature selection for continuous data classification using neighbourhood rough sets. Expert Systems with Applications, pp. 121765. DOI: https://doi.org/10.1016/j.eswa.2023.121765.
12. **Sun, Y., Pei, J. (2023).** Band selection based on hyperspectral piling fisher graphs (hspfigs) analysis. Infrared Physics and Technology, Vol. 133, pp. 104754. DOI: https://doi.org/10.1016/j.infrared.2023.104754.
13. **Wang, J., Tang, C., Zheng, X., Liu, X., Zhang, W., Zhu, E. (2022).** Graph regularized spatial-spectral subspace clustering for hyperspectral band selection. Neural Networks, Vol. 153, pp. 292–302. DOI: https://doi.org/10.1016/j.neunet.2022.06.016.
14. **Wang, J., Xu, P., Ji, X., Li, M., Lu, W. (2023).** Mic-shap: An ensemble feature selection method for materials machine learning. Materials Today Communications, Vol. 37, pp. 106910. DOI: https://doi.org/10.1016/j.mtcomm.2023.106910.
15. **Xie, F., Li, F., Lei, C., Yang, J., Zhang, Y. (2019).** Unsupervised band selection based on artificial bee colony algorithm for hyperspectral image classification. Applied Soft Computing, Vol. 75, pp. 428–440. DOI: https://doi.org/10.1016/j.asoc.2018.11.014.

ISSN 2007-9737

Article received on 12/07/2024; accepted on 17/01/2025.
**Corresponding author is Seyyid Ahmed Medjahed.*